Supplementary Information

Thermodynamically driven self-formation of copper-embedded nitrogen-doped carbon nanofiber catalysts for a cascade electroreduction of carbon dioxide to ethylene

Jae-Chan Lee,[a] Ji-Yong Kim,[a] Won-Hyo Joo,[a] Deokgi Hong,[a] Sang-Ho Oh,[a] Beomil Kim, [b] Gun-Do Lee, [a] Miyoung Kim, [a] Jihun Oh,[b, *] and Young-Chang Joo[a, *]

[a]*Department of Materials Science & Engineering, Seoul National University, Seoul 151-744, Korea*

[b]*Department of Materials Science and Engineering, Korea Advanced Institute of Science and Technology (KAIST), Daejeon 305-701, Korea*

***Corresponding authors:**

Jihun Oh*

E-mail: jihun.oh@kaist.ac.kr, Tel: +82-42-350-1726

Daehak-ro, Yuseong-gu, Daejeon 305-701, Korea

Young-Chang Joo*

E-mail: ycjoo@snu.ac.kr, Tel: +82-2-880-8986, Fax: +82-2-883-8197

1 Gwanak-ro, Gwanak-gu, Seoul 151-744, Korea

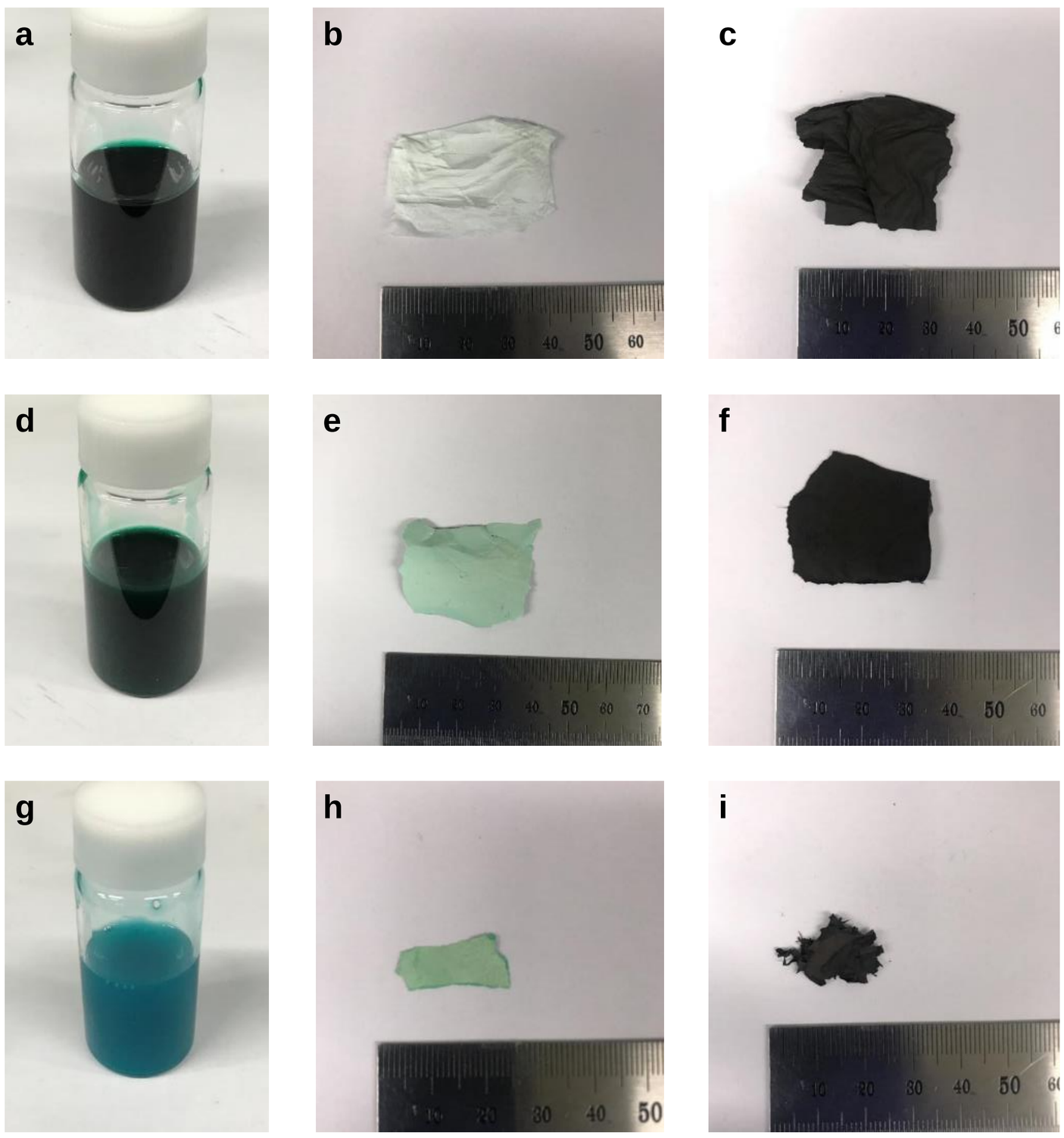

Fig. S1 Digital images of (a, d, g,) electrospinning solution, (b, e, h) as spun nanofibers, and (c, f, i) calcinated nanofibers of (a, b, c) Cu30/N-CNF, (d, e, f) Cu50/N-CNF, and (g, h, i) Cu50/CNF

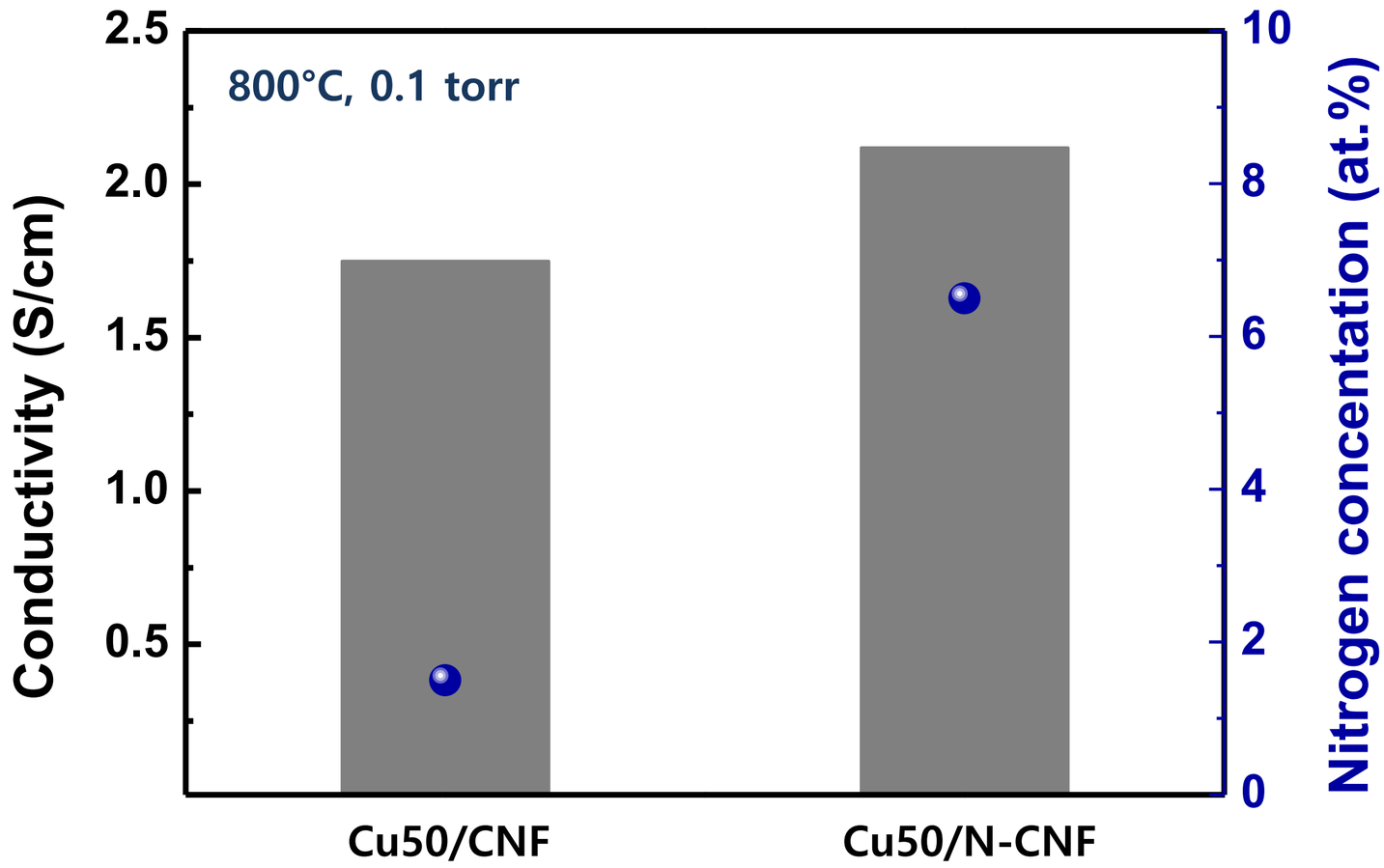

Fig. S2 Electrical conductivity and nitrogen concentration of Cu50/CNF and Cu50/N-CNF catalysts

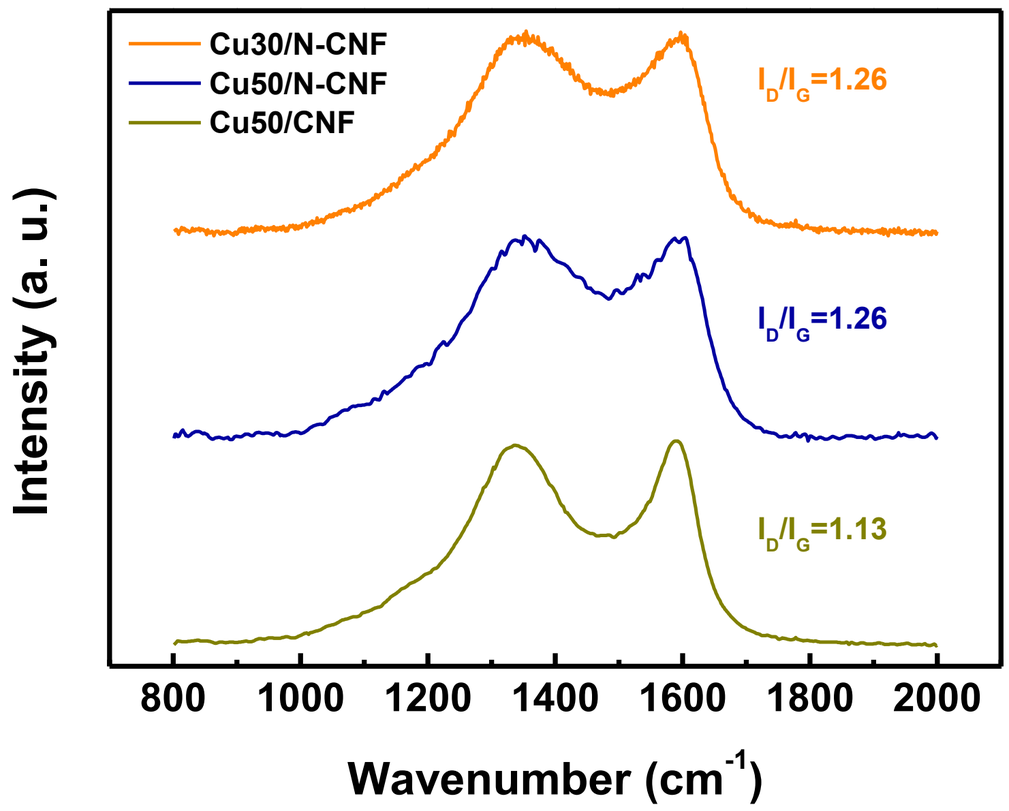

Fig. S3 Raman spectrum of Cu30/N-CNF, Cu50/N-CNF, and Cu50/CNF catalyst

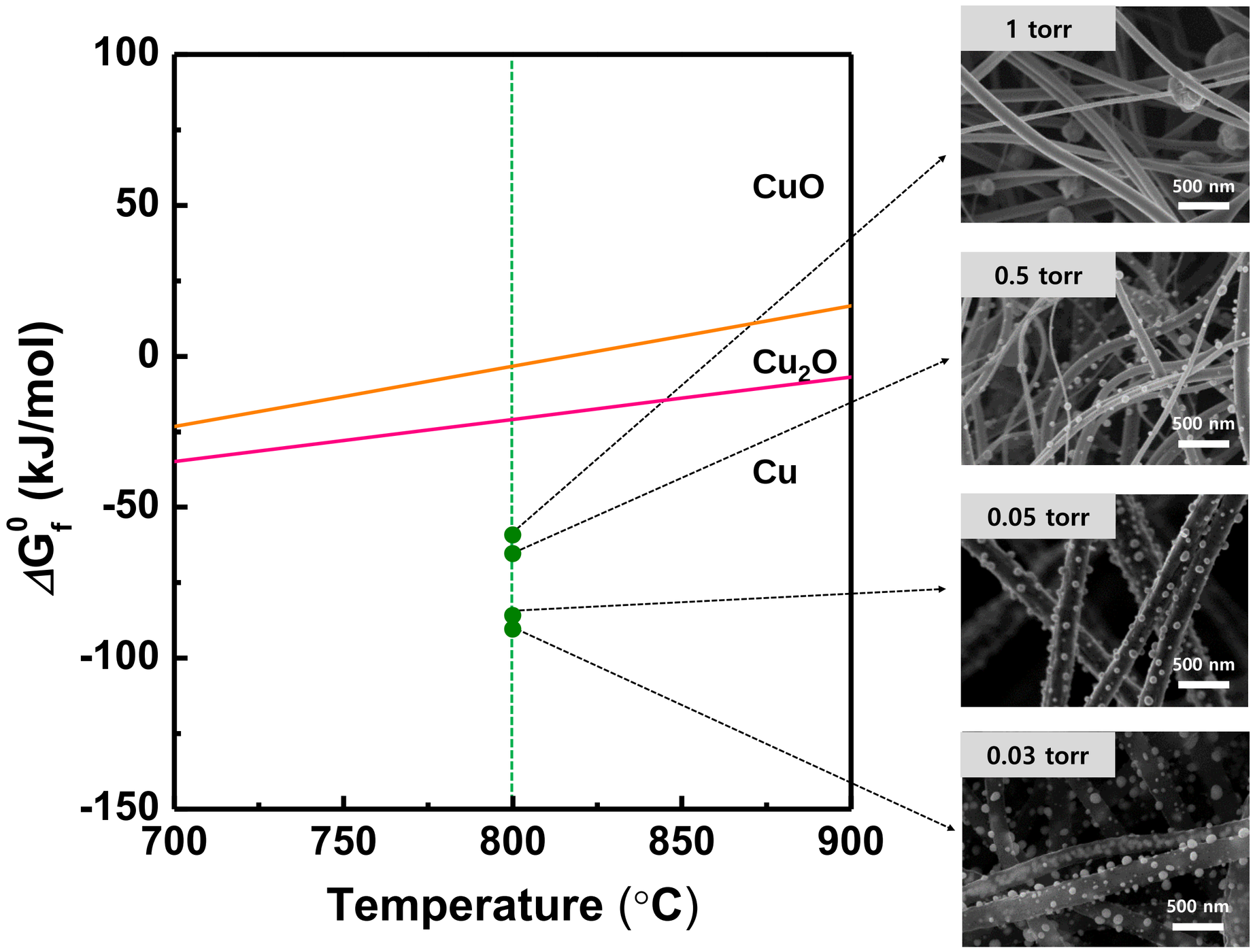

Fig. S4 Ellingham diagram of N, C, and Cu and morphological change of Cu50/N-CNF as O_2 partial pressure increases

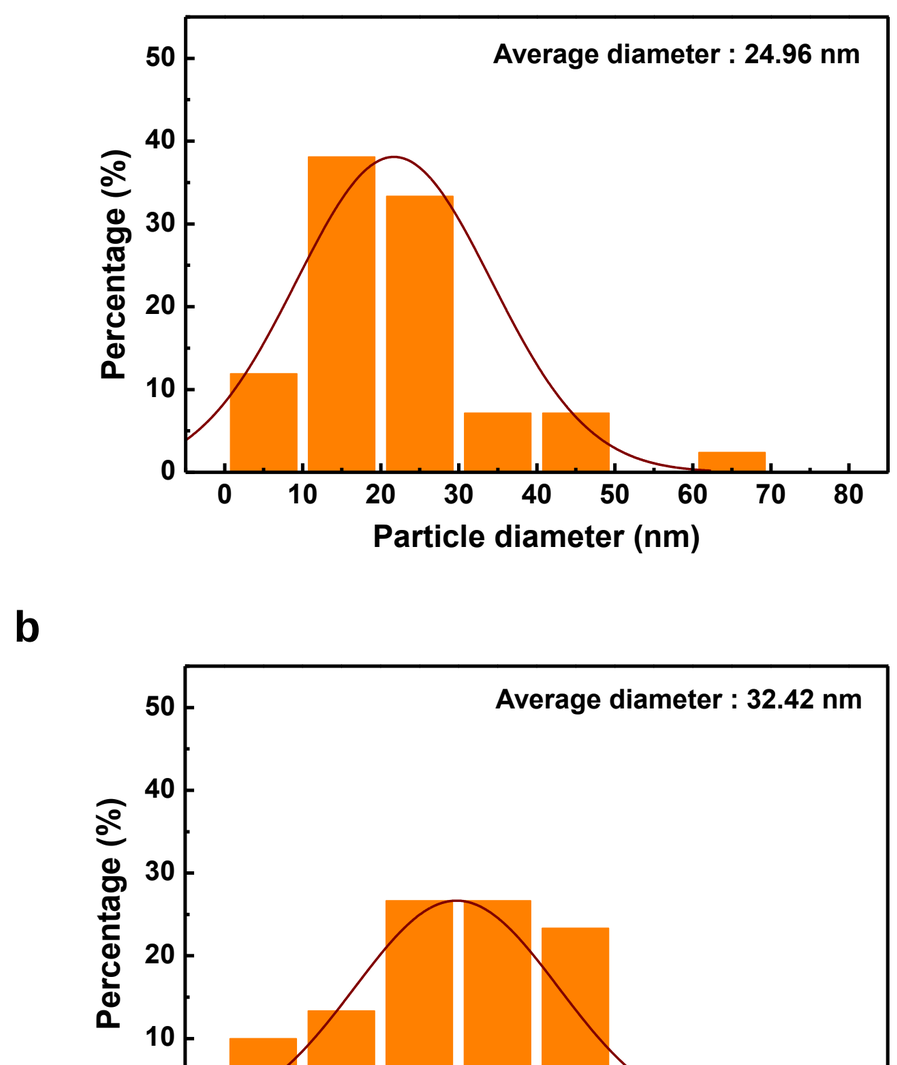

Fig. S5 Particle size distribution of (a) Cu30/N-CNF and (b) Cu50/N-CNF, and (c) Cu50/CNF

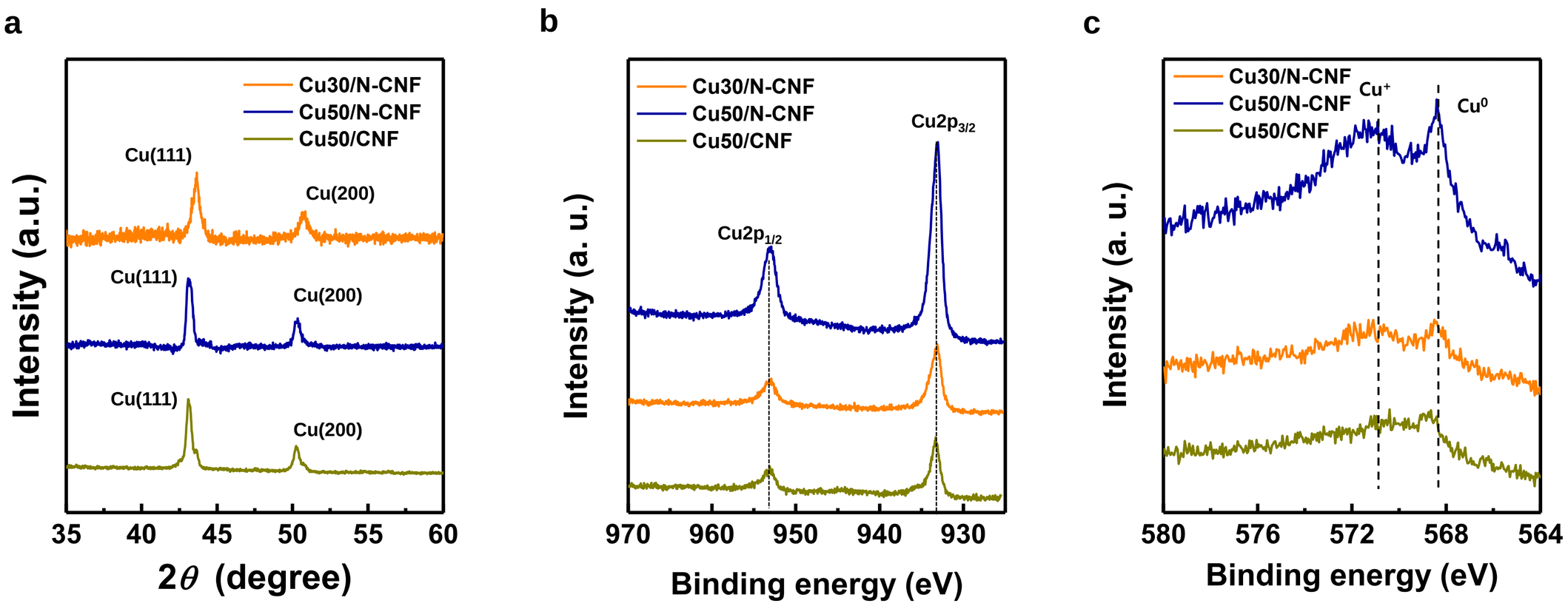

Fig. S6 (a) XRD pattern (b) Cu2p spectra, and (c) Cu LMM spectra of Cu/N-CNF catalysts

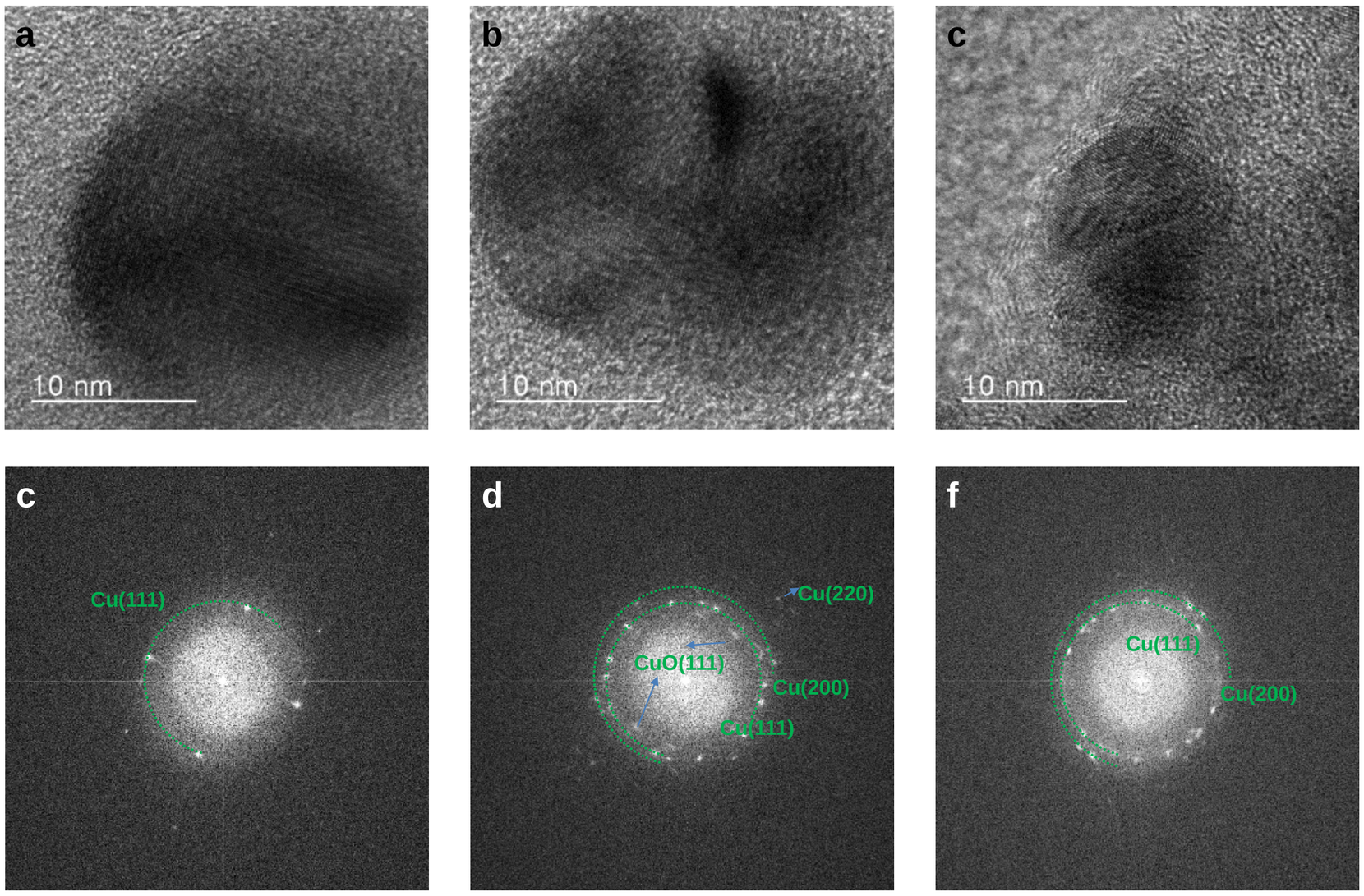

Fig. S7 HRTEM image and FFT diffraction pattern of (a, c) Cu30/N-CNF, (b, d) Cu50/N-CNF, and (c, f) Cu50/CNF

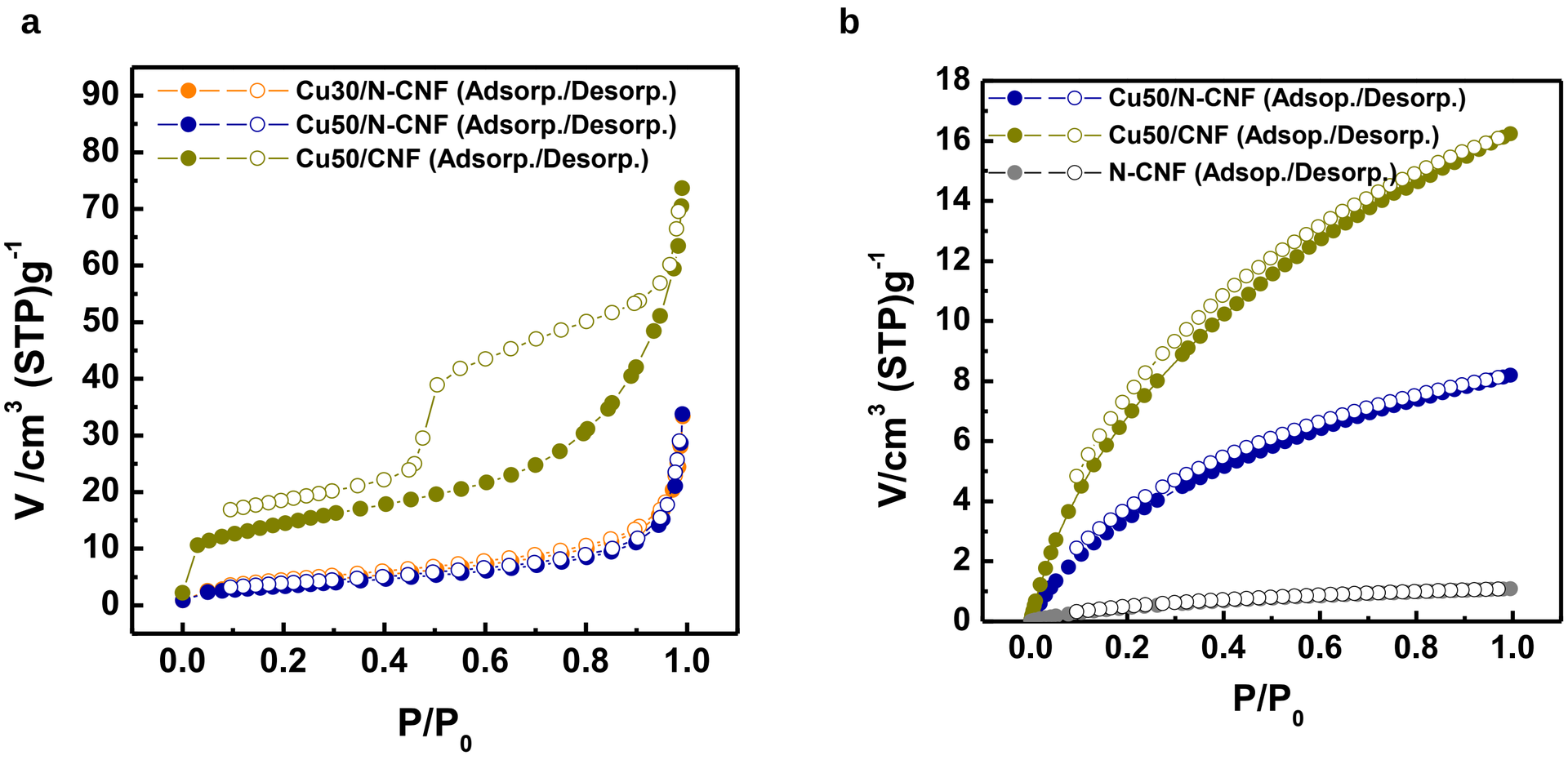

Fig. S8 Brunauer-Emmett-Teller (BET) specific surface area measured by (a) N_2 and (b) CO_2 gas.

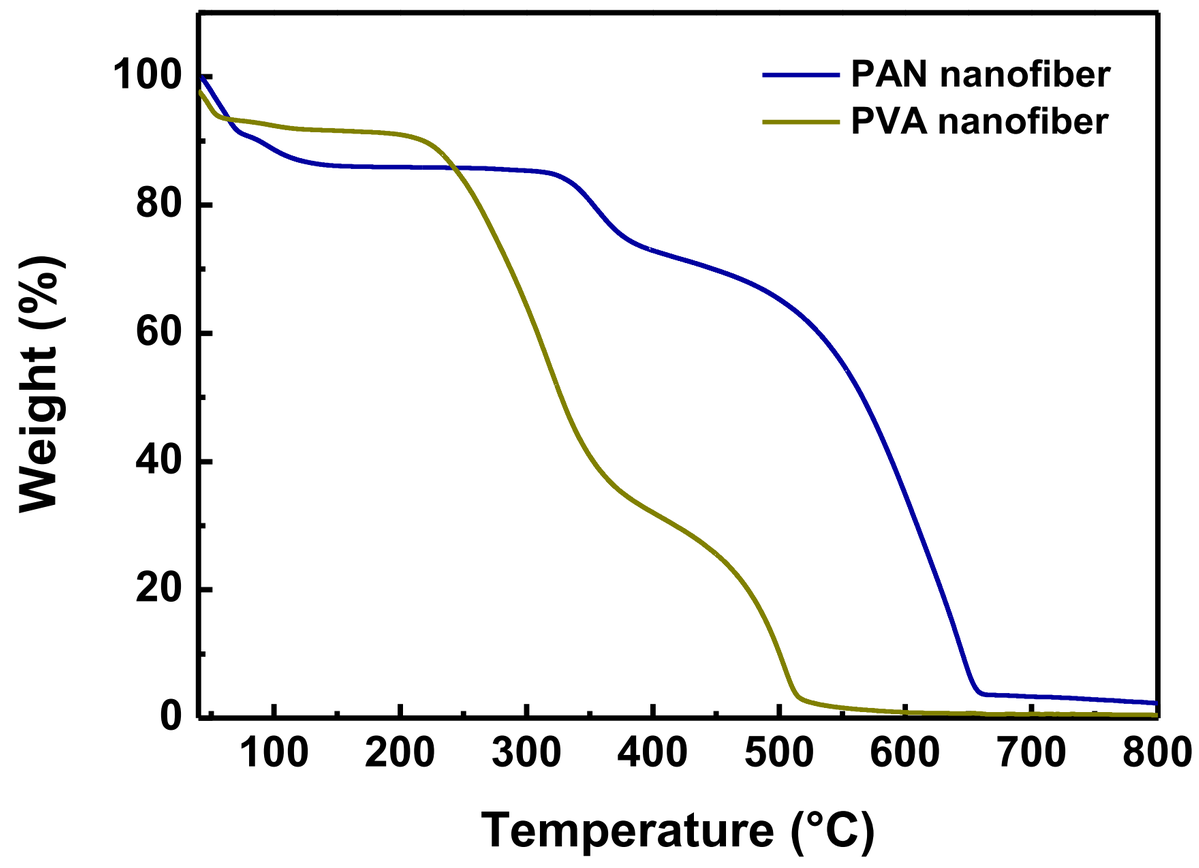

Fig. S9 TGA curves of PAN and PVA nanofibers.

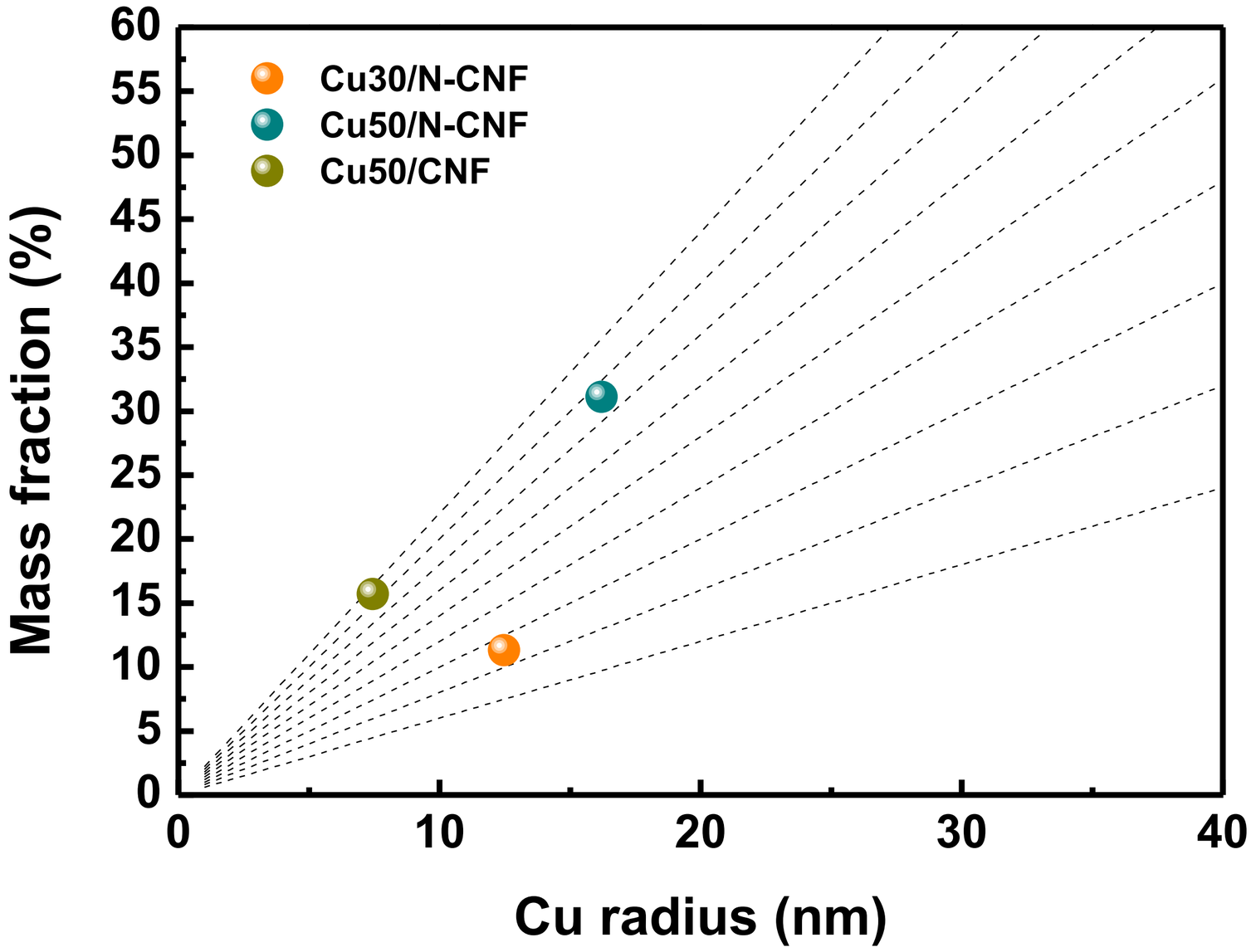

Fig. S10 Map of Cu radius – Cu mass fraction of Cu/(N)-CNF catalyst.

Assuming that the copper particle is sphere, surface area of copper particle and mass of copper are given as below: (n = The number of particles, r = Radius of copper particle, S = total surface area of copper particle, μ = Density of copper, α = Mass fraction of copper, M = Mass of catalyst)

$$S = n(4\pi r^2) \qquad \text{(Eq. 1)}$$

$$M_\alpha = n\mu\left(\frac{4}{3}\pi r^3\right) = \alpha M \qquad \text{(Eq. 2)}$$

and Eq. 3 can be derived by Eq. 2. Moreover, Eq.4 and Eq.5 formed by Eq. 1 and Eq. 3 which is derived by Eq.2 as follows:

$$n = \frac{3\alpha M}{4\mu\pi r^3} \qquad \text{(Eq. 3)}$$

$$S = \frac{3\alpha M}{\mu r} \qquad \text{(Eq. 4)} \qquad \alpha = \left(\frac{\mu S}{3M}\right) r = kr \qquad \text{(Eq. 5)}$$

When we plot the mass fraction of copper and radius of copper particle, it is confirmed that the slope is proportional to the total surface area of copper particle.

$$k = \frac{\mu}{3M} S \qquad \text{(Eq. 6)}$$

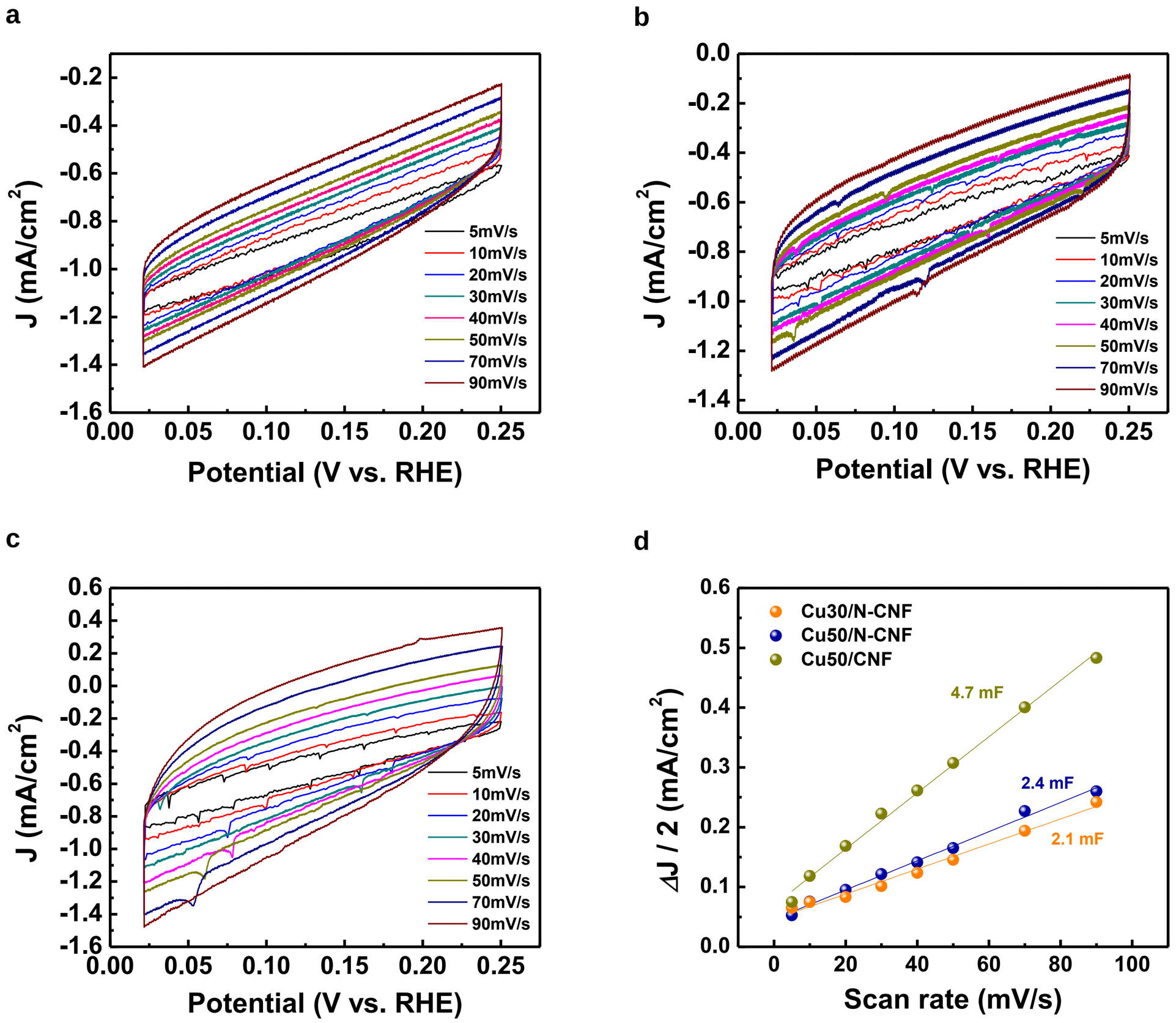

Fig. S11 Cyclic voltammograms of (a) Cu30/N-CNF, (b) Cu50/N-CNF, and (c) Cu50/CNF, and (d) determination of double layer capacitance of Cu30/N-CNF, Cu50/N-CNF, and Cu50/CNF.

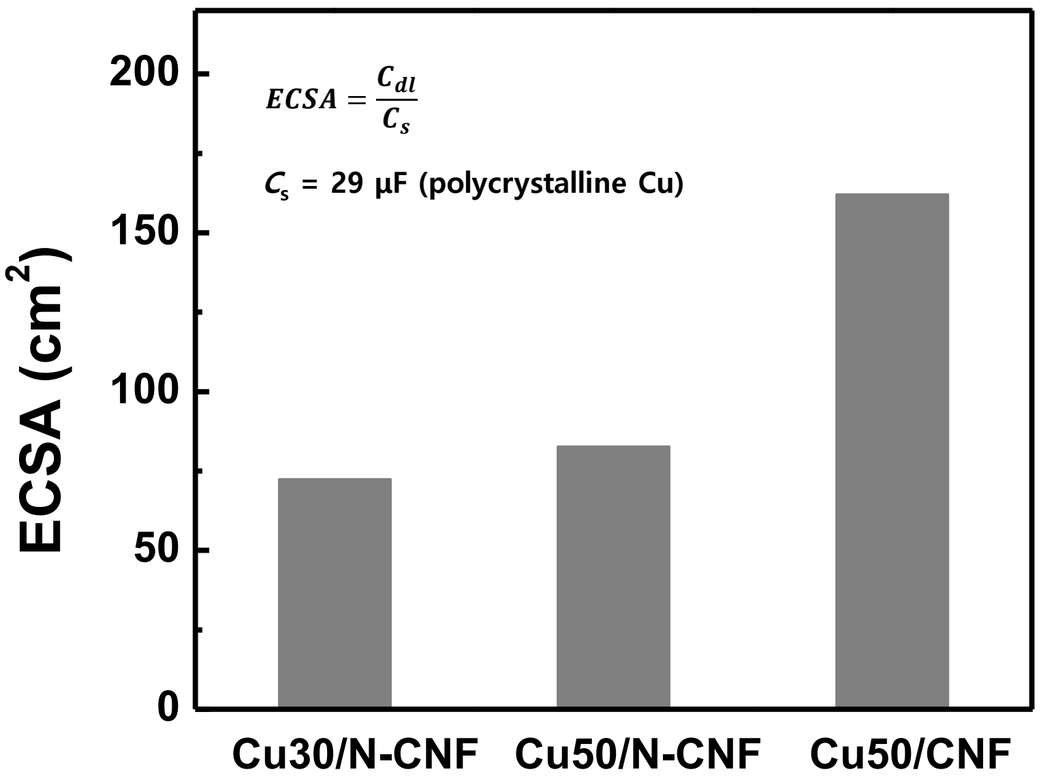

Fig. S12 Electrochemical surface area of Cu/N-CNF and Cu/CNF catalysts

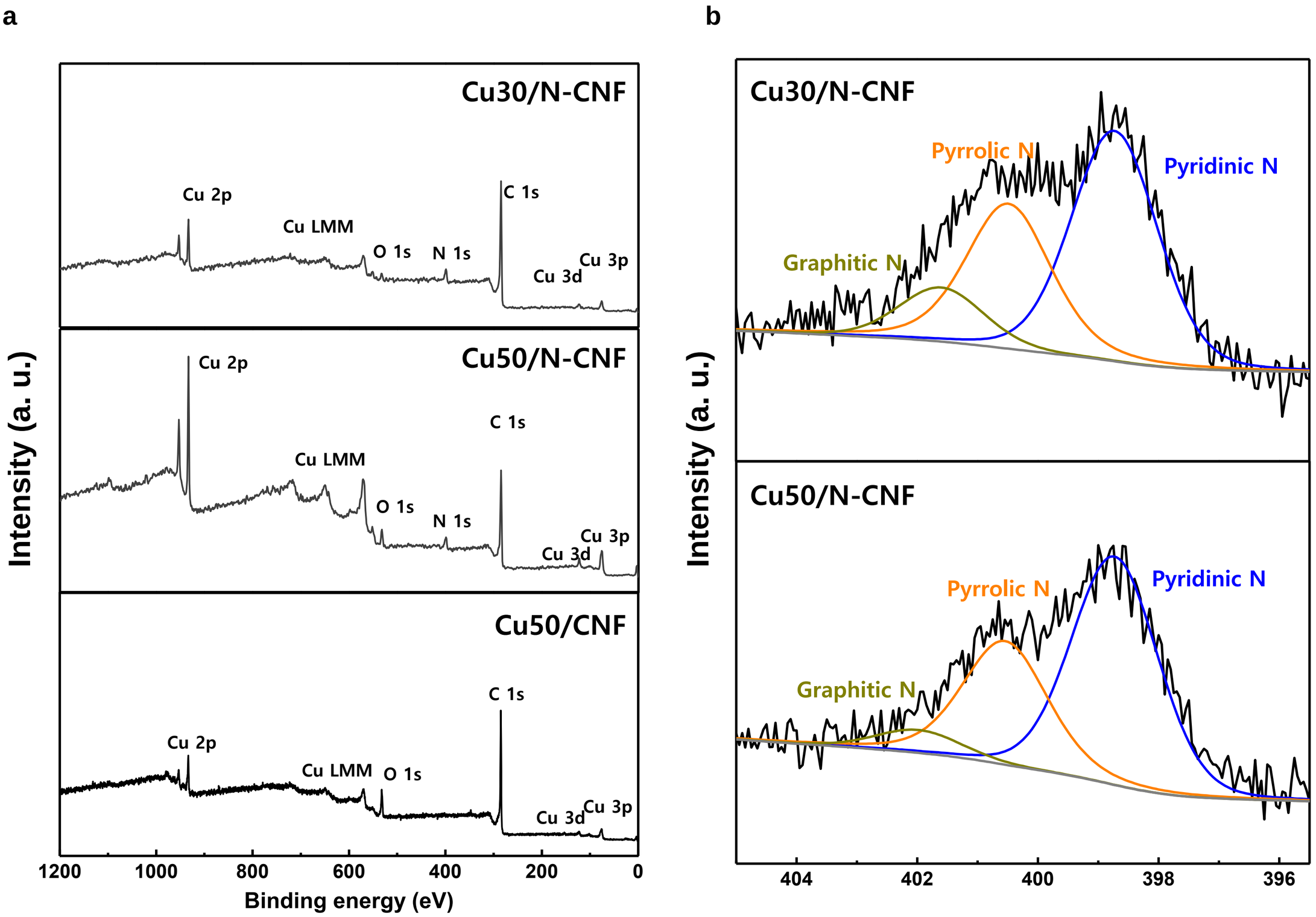

Fig. S13 (a) XPS survey spectra, (b) deconvolution of XPS N1s spectra of Cu30/N-CNF and Cu50/N-CNF, and (c) pyridinic N/Cu ratio of Cu30/N-CNF, Cu50/N-CNF

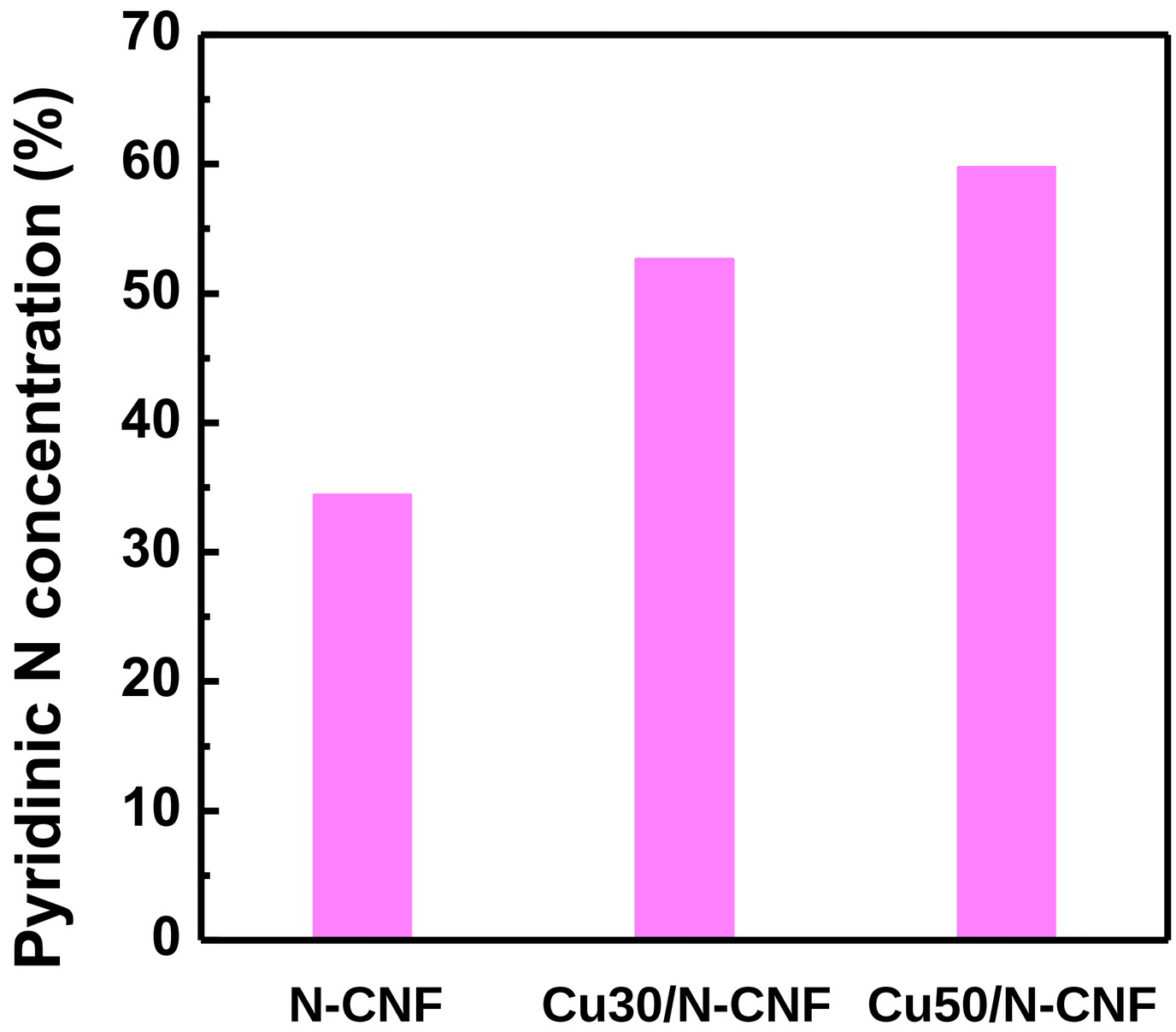

Fig. S14 Pyridinic N concentration of N-CNF, Cu30/N-CNF, and Cu50/N-CNF catalysts

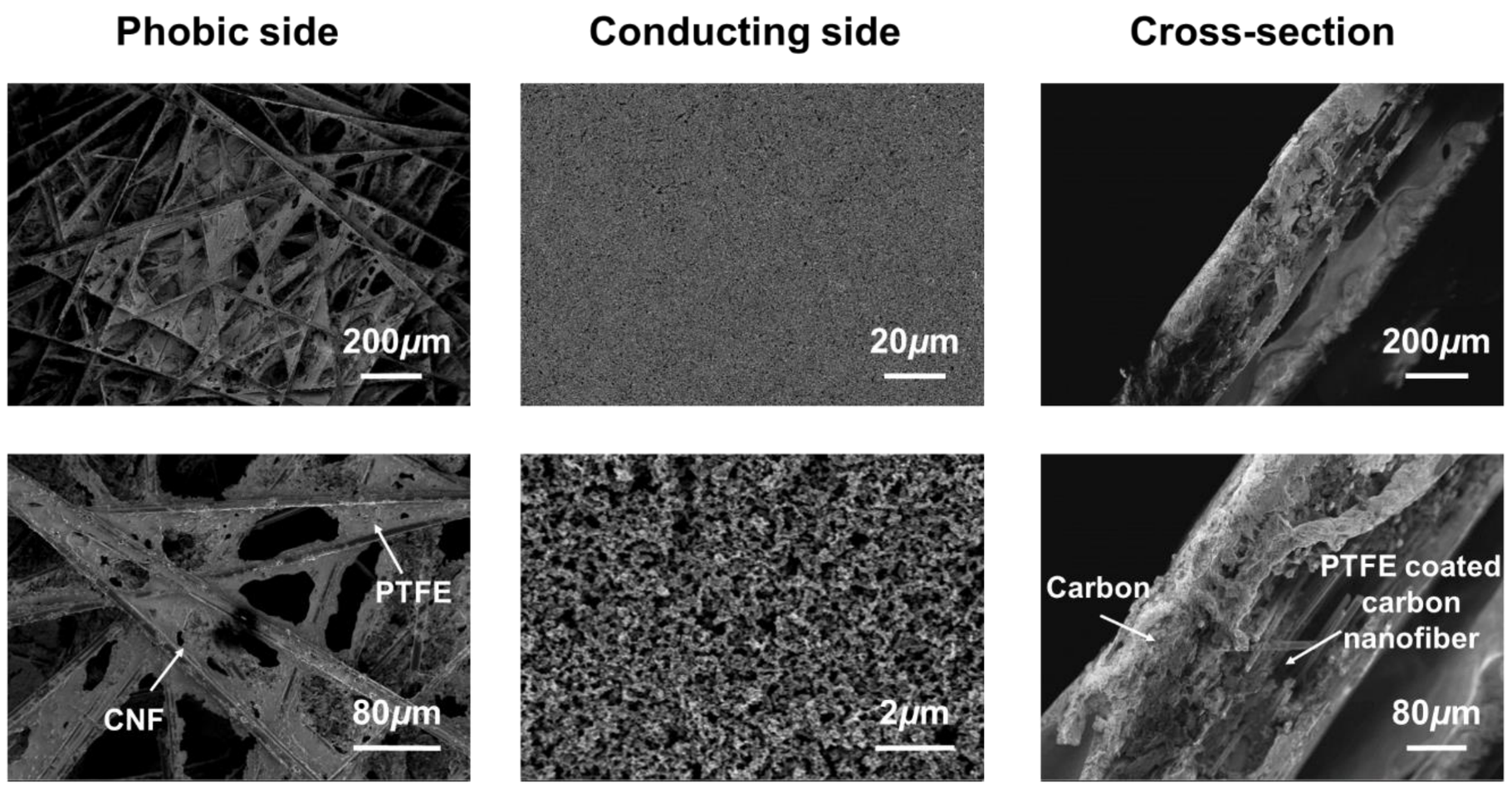

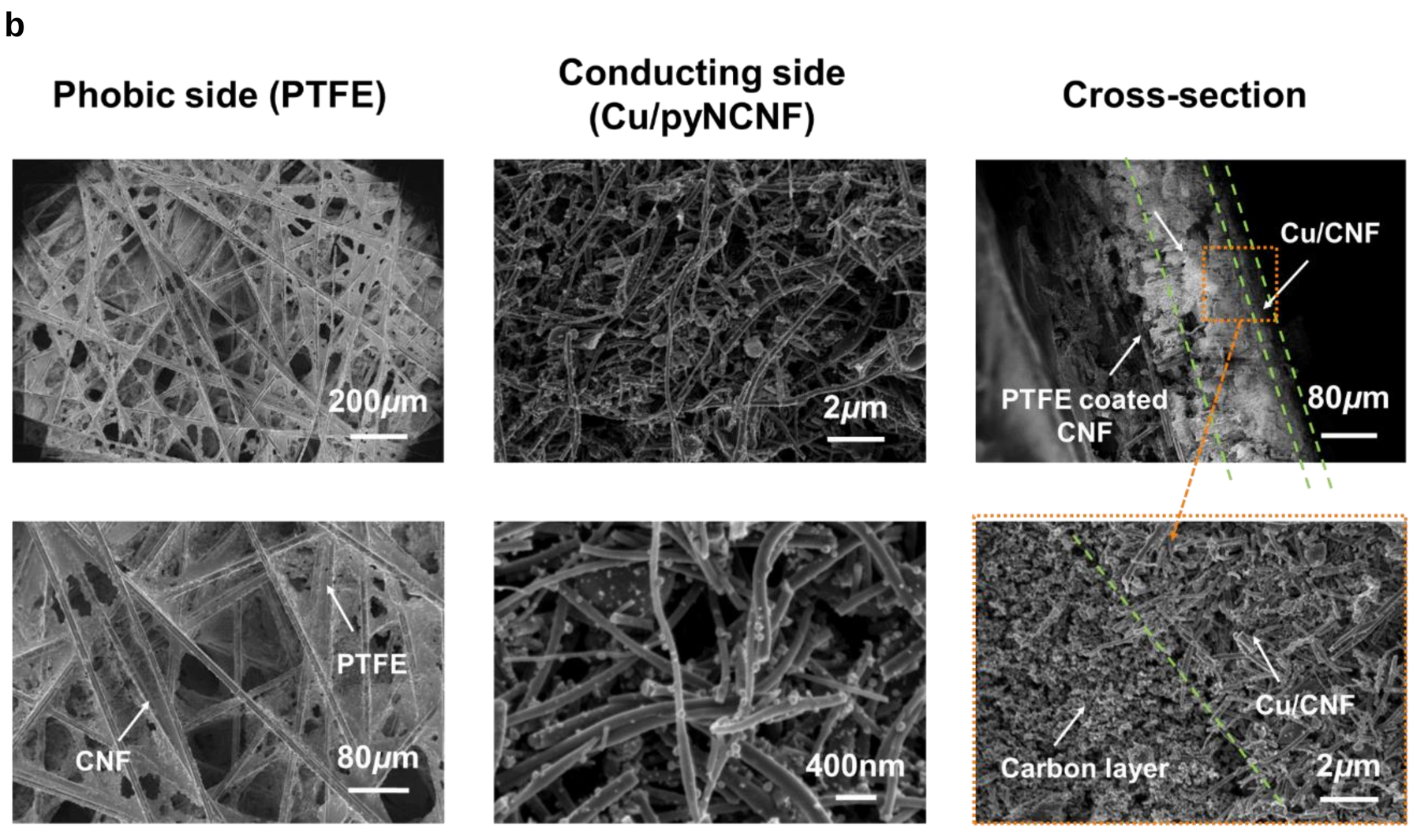

Fig. S15 SEM images of (a) bare and (b) Cu50/N-CNF coated GDE

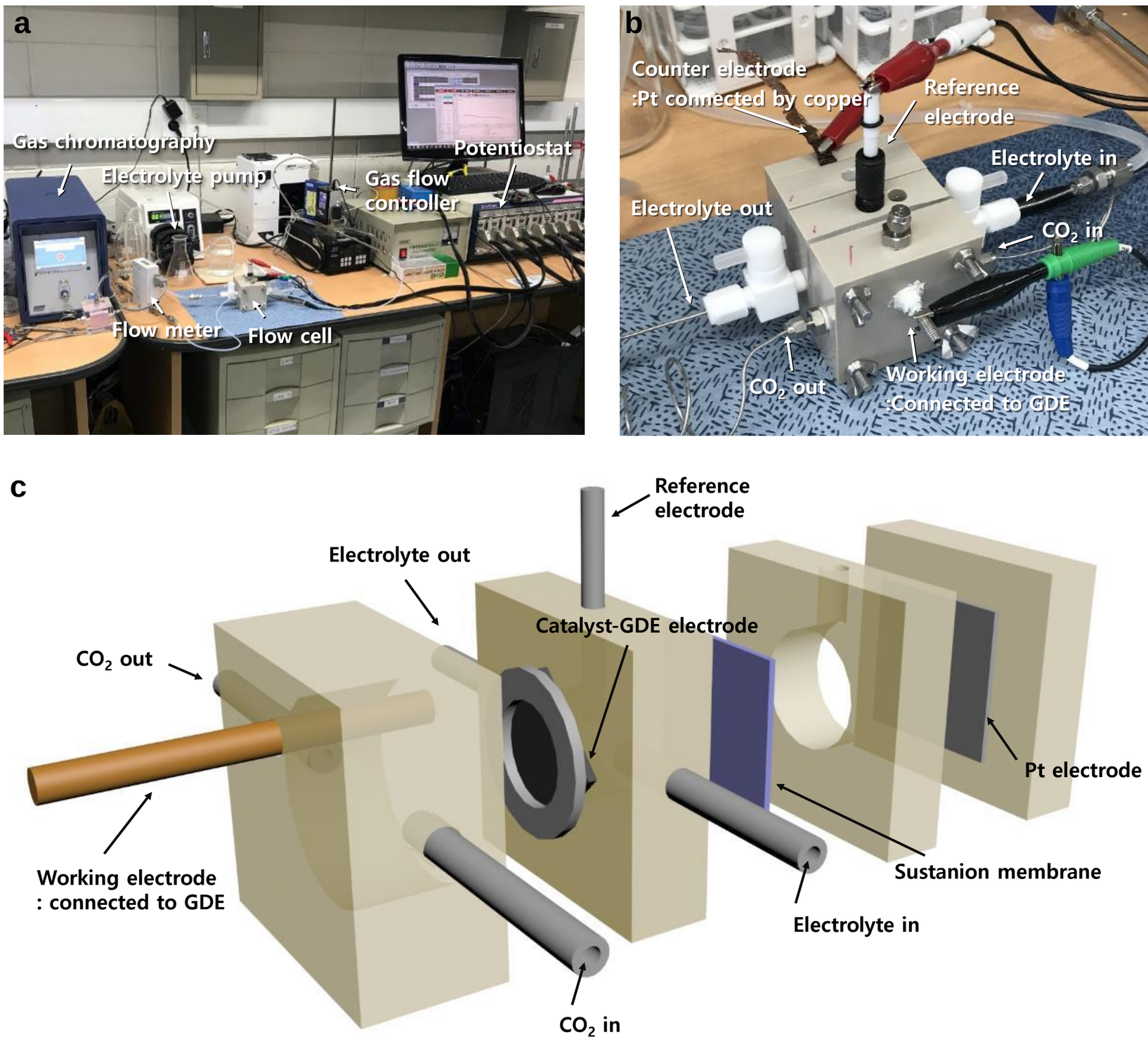

Fig. S16 Images of (a) CO_2 reduction system and (b) flow cell reactor. (c) Schematics of flow cell reactor for electrochemical CO_2 reduction system

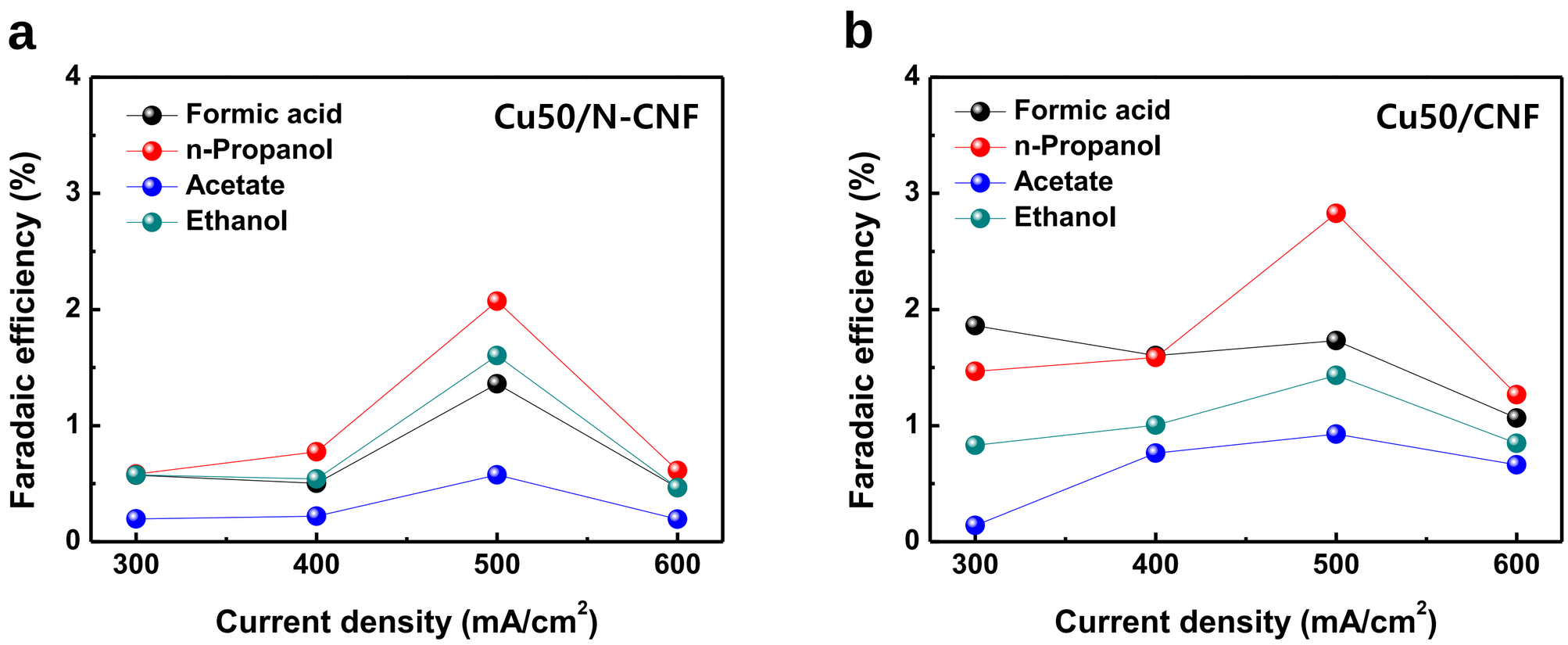

Fig. S17 Faradaic efficiency of liquid products during CO_2RR by (a) Cu50/N-CNF and (b) Cu50/CNF catalyst

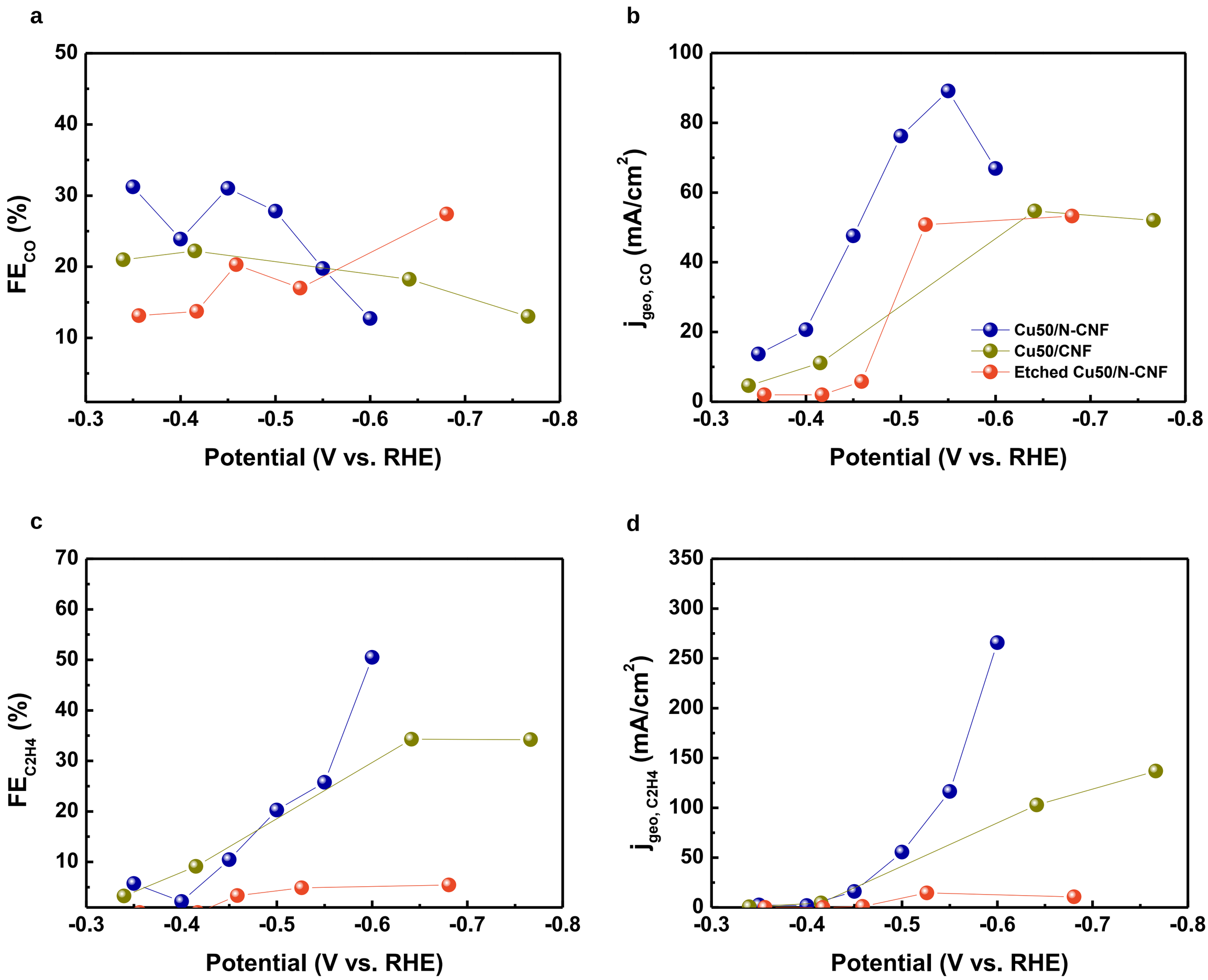

Fig. S18 (a,c) Faradaic efficiency and (b,d) geometric partial current density of (a, b) CO and (c, d) C_2H_4 as a function of potential

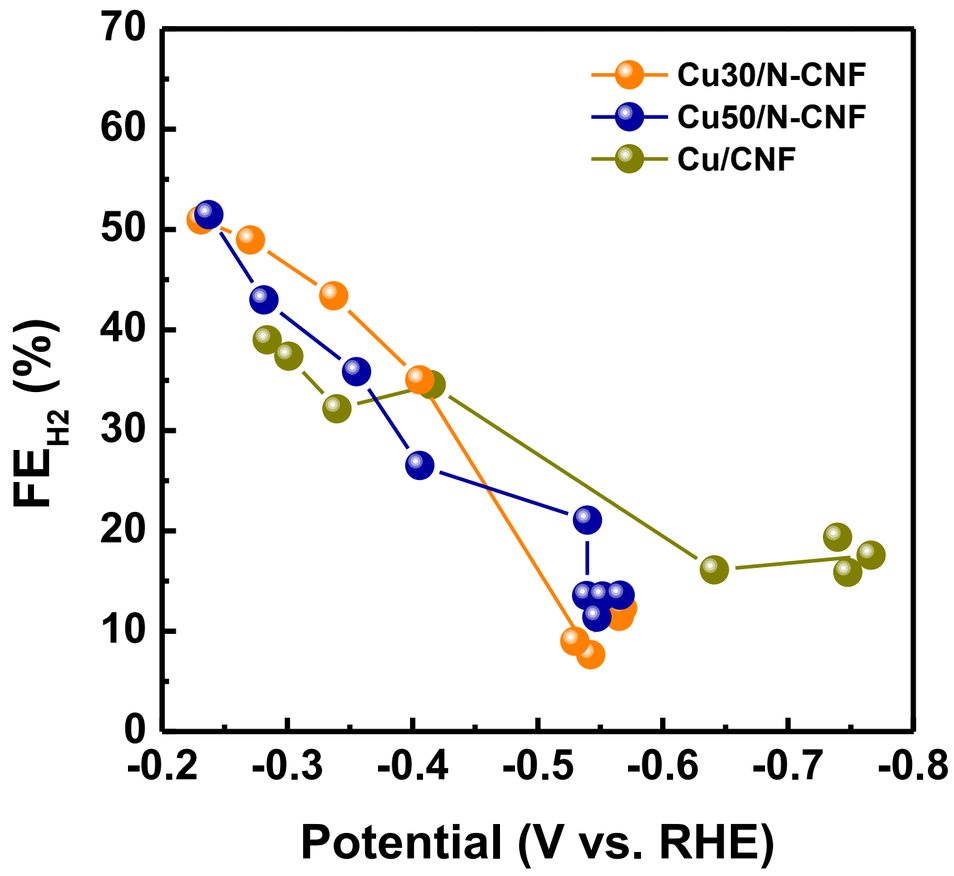

Fig. S19 Faradaic efficiency of H_2 as function of potential.

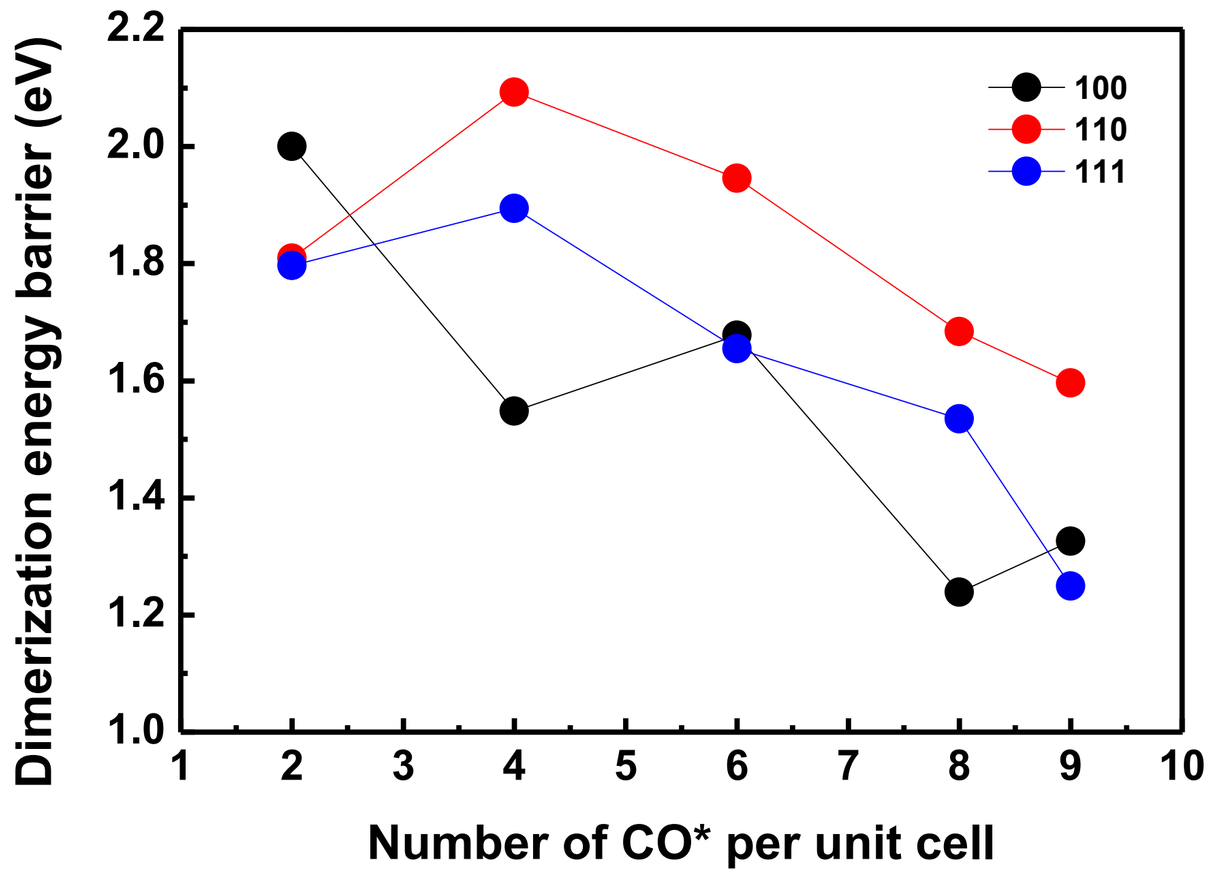

Fig. S20 Dimerization energy barrier as function of number of CO* per unit cell

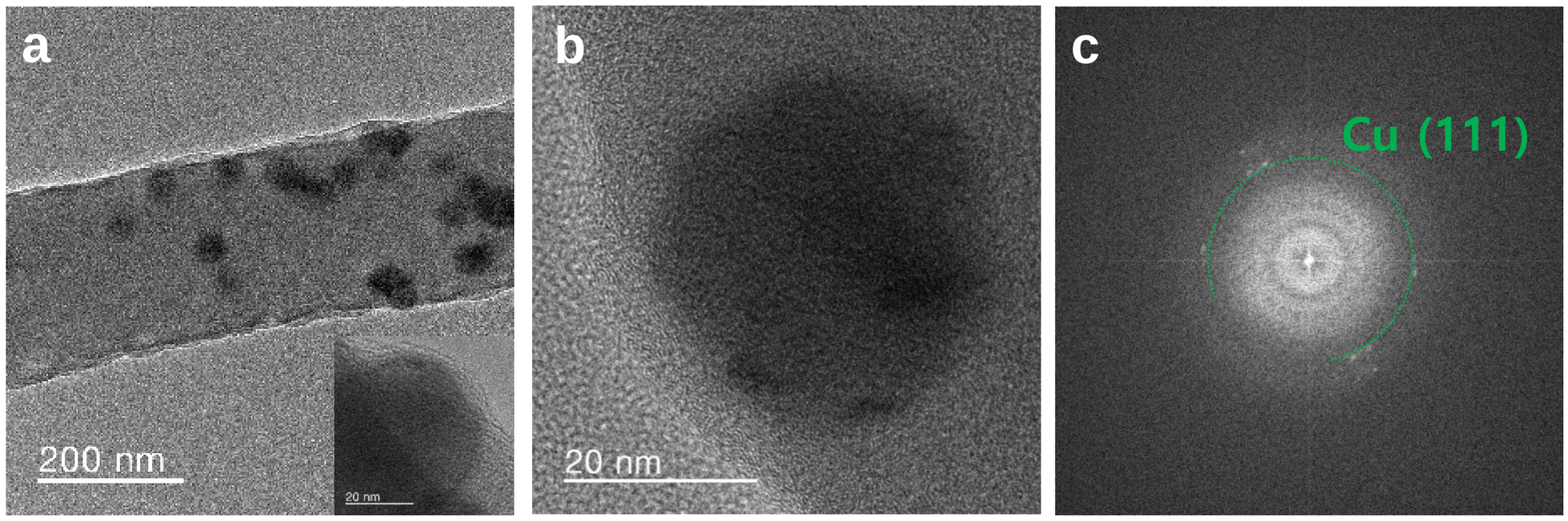

Fig. S21 (a, b) HRTEM image and (c) FFT analysis of Cu50/N-CNF after 2 hour of CO_2 RR

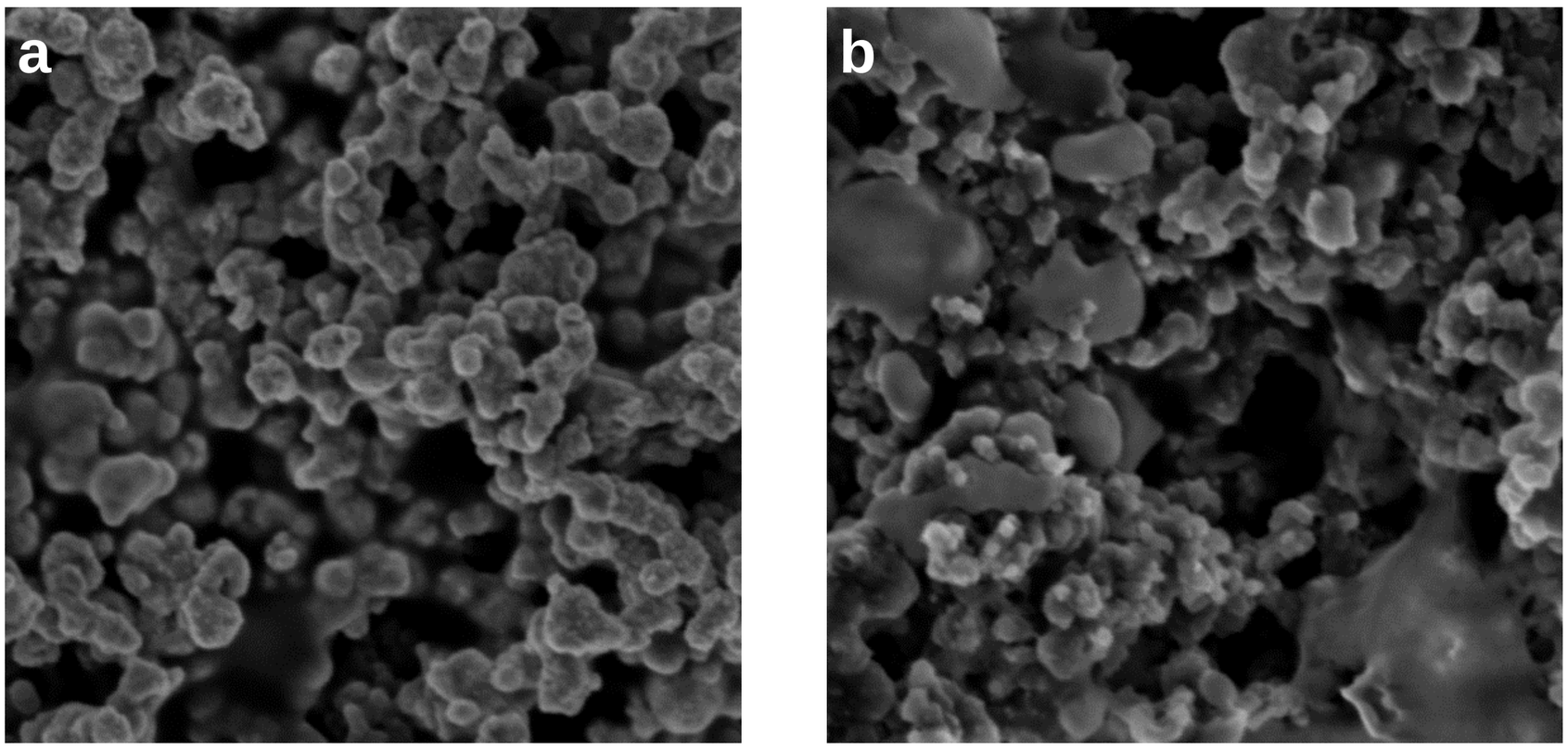

Fig. S22 SEM image of commercial Cu powder (a) before reaction, and (b) after 2 hour of CO_2 RR

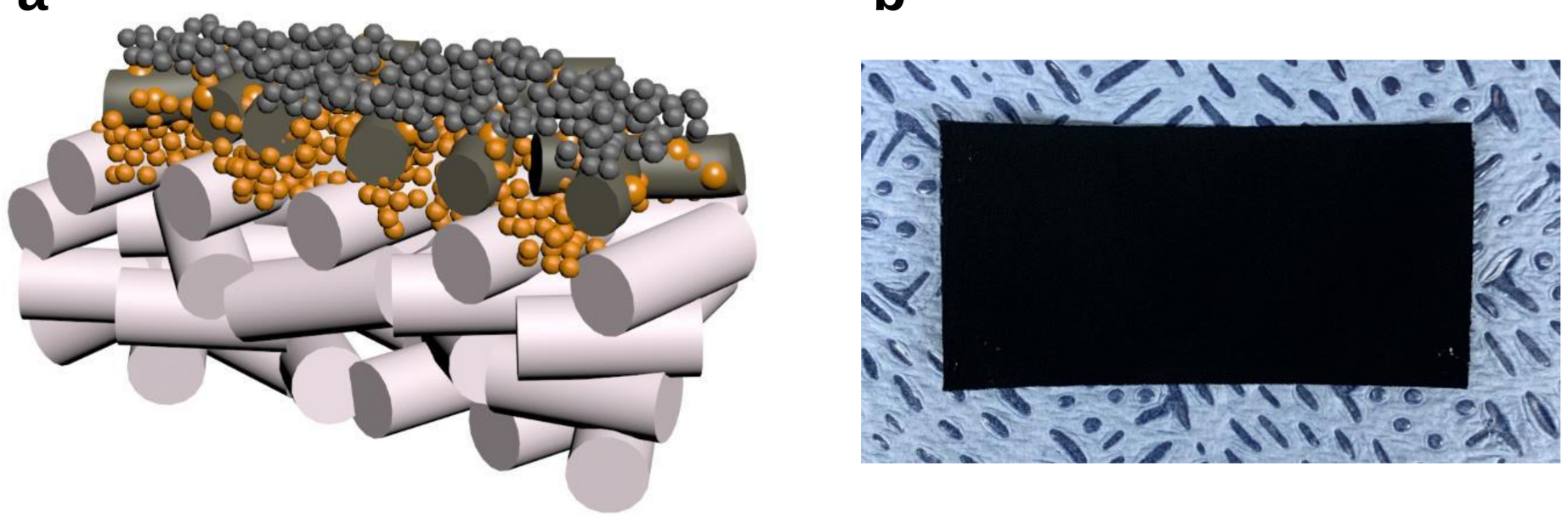

Fig S23 (a) Schematics and (b) image of carbon black/Cu/CuNCNF/PTFE

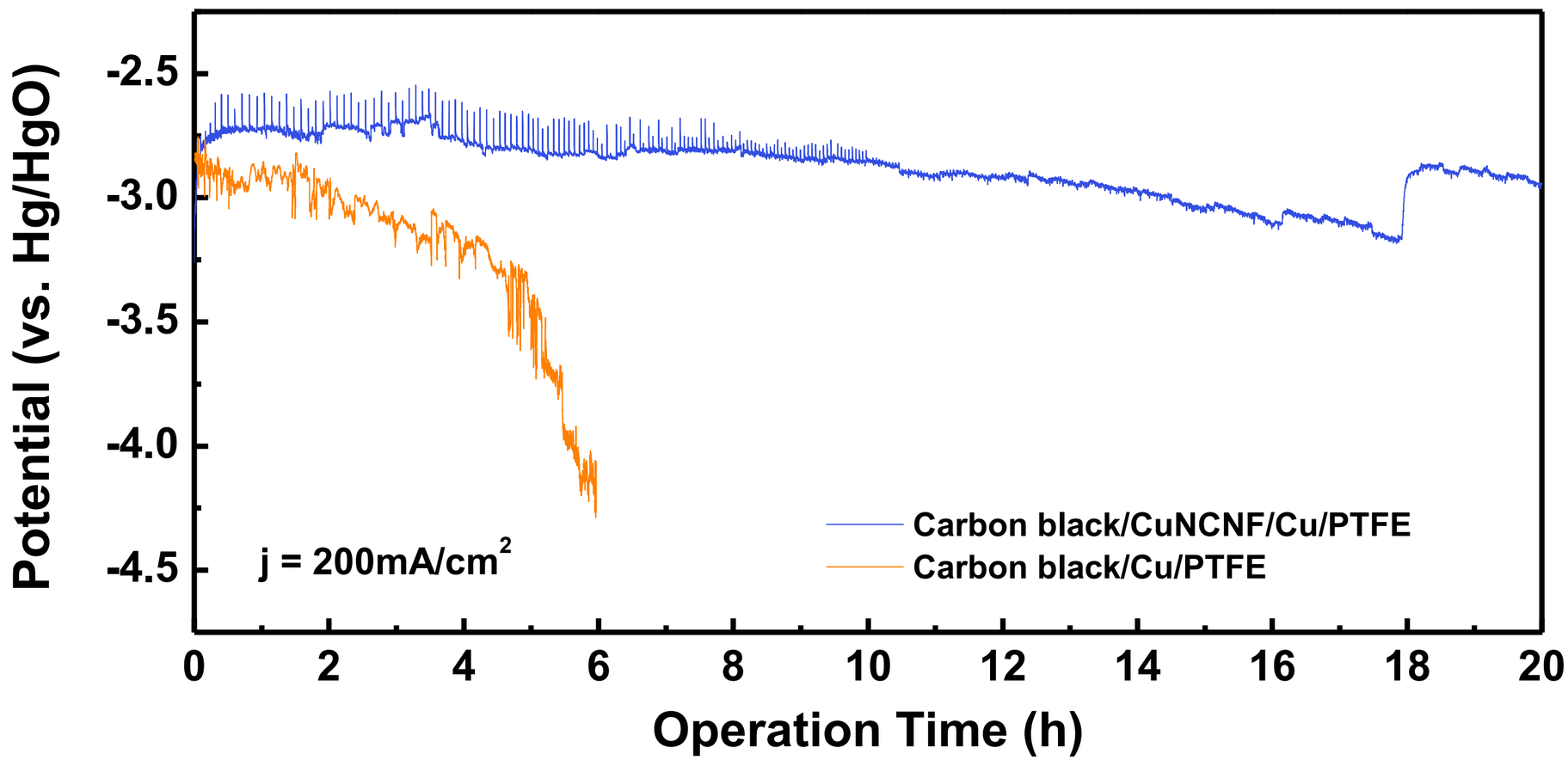

Fig. S24 Potential profile of carbon black/CuNCNF/Cu/PTFE and carbon black/Cu/PTFFE for 20 hours of reactions.